100% Converter-Interfaced Generation using Virtual Synchronous Generator Control: A Case Study based on the Irish System

Junru Chen*, Muyang Liu, Federico Milano, and Terence O'Donnell

University College Dublin

Abstract

The increase in the use of Converter-Interfaced Generation (CIG) in the power system will require these generators to not only feed the power but also establish the voltage and maintain the grid stability. Virtual Synchronous Generator (VSG) control of the CIG is proposed to fulfill this requirement since it mimics the dynamics of synchronous generation. This paper takes the all-Island Irish transmission system as an example to investigate the frequency stability of the system as it migrates towards 100% CIG under VSG control and quantifies the minimum conditions for frequency support to sustain the system under 100% CIG. Simulations are carried out considering the worst contingency in the Irish grid which is the loss of largest infeed, namely, the disconnection of the HVDC interconnector to the UK. The results are compared and discussed considering other scenarios that include primary frequency control of conventional power plants.

Keywords—Virtual Synchronous Generator (VSG), Frequency Control, Converter-Interfaced Generation (CIG), All-Island Irish Transmission System (AIITS), 100% Penetration.

1 Introduction

1.1 Motivation

Operating an entire national system with 100% converter-interfaced generation (CIG) and, hence, zero inertia, has not yet been implemented in practice but is an

*Corresponding author, email: junru.chen.1@ucdconnect.ie

expected scenario for the near future [1-4]. As discussed in [5] this requires CIG controls to implement grid forming capabilities. However, there is a lack of studies on the dynamic performance of a realistic power system as conventional Synchronous Generators (SG) are replaced by a specific CIG, i.e. Virtual Synchronous Generator (VSG), leading to a fully non-synchronous system. This paper aims at filling this gap.

1.2 Literature review

Conventionally, CIG has been controlled to be grid-following, where the converter is controlled as a current source, using a Voltage Source Converter (VSC) synchronized and following the grid frequency through a Phase-Locked Loop (PLL). Voltage and frequency support can be added to these grid following controls. Frequency support can be provided in the form of a droop control (proportional to frequency deviation) or a virtual inertia control (proportional to Rate of Change of Frequency). Frequency droop support alone cannot ensure the system stability when the system migrates to higher level of the CIG penetration, as the possibility of large RoCoF may cause relay trips after a contingency [6]. To avoid such instability, the provision of the virtual or emulated inertia from the CIG is required [7]. In the case of grid-following converters, several methods have been proposed. Deloaded operation of the CIG is a method used to reserve a certain amount of the available power by purposely shifting the CIG operating point from its optimum [8, 9]. Obviously, this shifting leads to the renewable energy waste and consequently results in economic losses for generator unless adequate compensation for such operation is provided. Alternatively, the inertia can be extracted from the rotating mass of the turbine by linking the speed of the turbine to the grid frequency in the machine side converter [10]. However, the kinetic energy released from the turbine reduces the rotor speed consequently resulting in generation reduction with a consequent energy recovery period and long-term operation will again lead to wind energy waste. To avoid such inevitable energy waste, the converter-interfaced electrical storage system [11] is widely recommended to be used as a “power sink” to store the energy in the over-generation case and release the energy in the under-generation case. The frequency

response of the storage connected grid-following converter can be achieved via a power compensation proportional to the Rate of Change of Frequency (RoCoF) measured by the PLL [12-15].

Nevertheless, even with the capability of grid following CIG to provide various forms of frequency support, as the penetration of CIG increases, in order to co-operatively establish the grid voltage in the absence of synchronous generation [5], converters have to move from the grid-following current-source mode to the grid-forming voltage-source mode. Some recent studies, e.g. from the MIGRATE project [16], suggest that at least 30% of the sources must be the grid-forming for the sake of the grid stability. The VSG control has been proposed to make the CIG behave like a voltage source while also providing primary frequency support and inertia into the system. Different VSG implementations have been proposed, e.g. the synchronverter [17, 18], virtual synchronous machine [19-21] and DC link capacitor-based VSG [22-24]. These VSG types mimic the behavior of the SG as their synchronization relies on the swing equation as opposed to a PLL. Studies have also looked at VSG controls applied to wind generation [25-27], PV generation [28, 29] and other distributed energy resources [30, 31]. These device-level studies of the VSG, including the topology and implementation have been well researched from the perspective of the power electronics. However, system level studies are still lacking, especially for the high level of the CIG penetration.

There have been several recent studies on low inertia systems, which have been studied either by purposely reducing the inertia constant of the SG present in the system or replacing the SG by CIG. However, reference [32], suggests that the study of the future CIG dominated system should use the latter method to accurately represent the effect of increased CIG penetration. Reference [33] compared several different forms of grid forming controls and their interactions with SGs, using detailed electromagnetic transient (EMT) system modeling in the IEEE 9-bus system. From this study the authors concluded that due to their faster response, grid forming

CIG can improve frequency stability metrics compared to the all SG system, especially if steps are taken to ensure they remain working in voltage source mode without current limitation. On the other hand, it has also been recognized that this fast response can give rise to higher frequency oscillations in the system through the interaction with line dynamics [34]. However, these higher frequency modes can be damped with for example the addition of a virtual resistance [35] and damping [36] in the grid-forming CIG. Voltage stability is also a concern in the migration to 100% CIG systems [37]. Reference [12], has indicated that smaller capacity distributed CIG may have benefits compared to larger capacity centralized CIG power plants, due to their ability to locally compensate reactive power. It should also be noted that it is possible to implement grid-forming controls which do not emulate inertia, such as droop controls [38] or power synchronization control [39]. The fast response achievable from CIG using such controls can achieve a stable frequency in the grid and the concept of inertia may be not needed. However, in the mid-term, since existing systems expect a slow frequency change, the concept of maintaining a virtual inertia may have operational advantages [5]. Note that this does not necessarily mean that the fast-acting capability of the CIG is not being utilized because, as shown in this work, the droop response can still be fast-acting thus giving advantages in terms of frequency stability.

Most of the system-level researches for the VSG have been applied in microgrids or test systems. For example, references [40,41] compare the VSG and droop control in terms of frequency dynamics and reference [42] uses bifurcation theory to analyze the stability in VSG-dominated microgrids. Reference [43] improves the VSG robustness and [44] enhances the VSG power sharing accuracy in the microgrid. Some works [45-48] have discussed the VSG performance based on the implementation in the IEEE standard test system models. For example, reference [45] analyzed the VSG small signal stability and [46,47] illustrate the VSG basic functions in the IEEE 39-bus system and [48] presents the VSG primary support

behavior in the IEEE 12-bus system.

Finally, some comment is perhaps necessary on the justification for the use of VSG control, which essentially mimics SG characteristics in an all CIG system where there is clearly no inherent physical link between supply-demand imbalance and frequency. In theory the frequency in such a system could be fixed at 50 Hz or 60 Hz (or indeed 0 Hz) by the converter controls. However, the question remains as to how to achieve load sharing between generators to satisfy the demand. It could be envisaged that this could be achieved by means of an extensive communication system, which of course raises further issues around security, reliability, etc. Therefore, even in the 100% CIG scenario, maintaining frequency as the means of communication for supply-demand imbalance would seem reasonable and even desirable. Hence the use of VSG control which links the CIG frequency to its loading so as to mimic the actions of an SG is an attractive solution, especially in the medium term where the system must work with a mix of CIG and conventional SGs.

1.3 Contributions

As discussed in the literature review above, the dynamic performance of single VSG devices has been tested only considering single-machine infinite-bus systems or stand-alone microgrids. No previous works focuses on a real-world power system with 100% VSG-controlled CIG. This raises several interesting issues, such as the frequency dynamics of such a system and the role of energy storage devices to provide the inertial response.

This paper investigates these issues by means of a case study on the All-island Irish Transmission System (AIITS), which is a real-world national power system operated with high penetration of CIG. In particular, the paper investigates the frequency stability and dynamics of the system as it migrates from the present situation towards 100% CIG. The VSG controlled CIG is assumed to come from stochastic wind generation combined with Electrical Energy Storage (ESS). Two different implementations of combining the storage with the wind generation is

considered, one where the storage is located in the DC link of the wind turbines and one where the storage is co-located, external to the wind turbines. The minimum ESS rating required in order to maintain the present stability level is investigated.

1.4 Organization

The remainder of this paper is structured as follows. Section II briefly reviews the VSG modeling and its operation. Section III introduces the dynamic model of the AIITS considered in the case study. Section IV analyzes the dynamic response of the system under a 100% CIG penetration following the worst-case contingency. The capacity of ESS required to maintain stability in the 100% CIG scenario is also evaluated. Section V analyzes the effect of the stochastic wind and demand on frequency dynamics. Finally, Section VI draws relevant conclusions.

2 Review of Virtual Synchronous Generator

VSG control has been extensively described in previous works and here we present only a brief overview of the aspects which are of particular relevance to this work. Here the VSG control is proposed to be embedded into the grid-tied VSC, where the DC bus is supplied by a power source which, as discussed later, is either renewable generation and/or ESS. The VSG applies the swing equation to determine the voltage phase angle with respect to the grid and voltage support to determine the voltage amplitude, thus, the VSC output voltage is directly controlled. The full details are given in [19,20,46] and here we briefly explain the structure which is described by the set of equations given by (1 - 10).

Assuming the DC link voltage of the VSG is fixed, the VSG control is an additional outer loop of the conventional outer voltage inner current control of the VSC as shown in Fig. 1. The core VSG control part contains three subparts, the active power regulation which determines voltage angle, the voltage regulation which determined voltage magnitude and the virtual impedance which can be used to alter the apparent output impedance. The active power regulation emulates the SG swing equation (1) with inertia M and damping D which provides synchronization of phase δ and

frequency ω_{VSG}. It also allows for turbine governor (TG) emulation (2) with active power droop computed from, K_d and the difference between the detected grid frequency ω_{pll} (detected by PLL) and the reference frequency ω^*. The voltage regulation part emulates the automatic voltage regulator (AVR) (3) with a compensation gain K_v to determine the emulated electric potential E. The virtual impedance allows for stator impedance emulation as a virtual impedance $r_v + j\omega_{VSG} l_v$ (4). The overall VSG control provides the reference voltage v_o^* to the conventional VSC, which is implemented with outer voltage (5) inner current (6) control and an LC filter (7,8), where K_{pv}/K_{iv} and K_{pc}/K_{ic} are the PI settings for the voltage and current control respectively, and l_f and b_f are the filter inductance and capacitance respectively. The output voltage v_o tracks the reference voltage which is connected to the grid with voltage V_g through the transmission line with its impedance $r_g + j\omega_{grid} l_g$ (9). The delivered power, P (10) feeds back into the swing equation and the grid voltage is supported by the AVR emulator. Therefore, equations (1~10) define the Differential-Algebraic Equation (DAE) model of the VSG where the equation correspond to the different blocks as indicated in Fig. 1.

$$\left.\begin{aligned} M\frac{d\Delta\omega_{VSG}}{dt} &= P^* + P_{droop} + D\Delta\omega_{VSG} - P \\ \dot{\delta} &= \Delta\omega_{VSG} \end{aligned}\right\} \quad (1)$$

$$P_{droop} = K_d(\omega^* - \omega_{pll}) \quad (2)$$

$$E = V^* + K_v\left(V^* - V_g\right) \quad (3)$$

$$\left.\begin{aligned} v_{od}^* &= E\cos\delta - i_d r_v + i_q \omega_{VSG} l_v \\ v_{oq}^* &= E\sin\delta - i_d \omega_{VSG} l_v - i_q r_v \end{aligned}\right\} \quad (4)$$

$$\left.\begin{aligned} i_{cvd}^* &= K_{pv}(v_{od}^* - v_{od}) + K_{iv}\varepsilon_d - \omega_{VSG} b_f v_{oq} \\ i_{cvq}^* &= K_{pv}\left(v_{oq}^* - v_{oq}\right) + K_{iv}\varepsilon_q + \omega_{VSG} b_f v_{od} \\ \dot{\varepsilon_d} &= v_{od}^* - v_{od} \\ \dot{\varepsilon_q} &= v_{oq}^* - v_{oq} \end{aligned}\right\} \quad (5)$$

$$\left.\begin{aligned} v_{cvd}^{*} &= K_{pc}(i_{cvd}^{*} - i_{cvd}) + K_{ic}\gamma_d - \omega_{VSG} l_f i_{cvq} \\ v_{cvq}^{*} &= K_{pc}\left(i_{cvq}^{*} - i_{cvq}\right) + K_{ic}\gamma_q + \omega_{VSG} l_f i_{cvd} \\ \dot{\gamma_d} &= i_{cvd}^{*} - i_{cvd} \\ \dot{\gamma_q} &= i_{cvq}^{*} - i_{cvq} \end{aligned}\right\} \quad (6)$$

$$\left.\begin{aligned} \frac{l_f}{\Omega_b}\frac{di_{cvd}}{dt} &= v_{cvd} - v_{od} - r_f i_{cvd} + \omega_{grid} l_f i_{cvq} \\ \frac{l_f}{\Omega_b}\frac{di_{cvq}}{dt} &= v_{cvq} - v_{oq} - r_f i_{cvq} - \omega_{grid} l_f i_{cvd} \end{aligned}\right\} \quad (7)$$

$$\left.\begin{aligned} \frac{b_f}{\Omega_b}\frac{dv_{od}}{dt} &= i_{cvd} - i_d + \omega_{grid} b_f v_{oq} \\ \frac{b_f}{\Omega_b}\frac{dv_{oq}}{dt} &= i_{cvq} - i_q - \omega_{grid} b_f v_{od} \end{aligned}\right\} \quad (8)$$

$$\left.\begin{aligned} \frac{l_g}{\Omega_b}\frac{di_d}{dt} &= v_{od} - V_g \cos(-\delta) - r_g i_d + \omega_{grid} l_g i_q \\ \frac{l_g}{\Omega_b}\frac{di_q}{dt} &= v_{oq} - V_g \sin(-\delta) - r_g i_q - \omega_{grid} l_g i_d \end{aligned}\right\} \quad (9)$$

$$P = i_d V_g \cos(-\delta) + i_q V_g \sin(-\delta) \quad (10)$$

2.1 VSG and Renewable Generation

VSG control can be viewed as an advanced droop control [41], which was initially proposed to be used to control storage to support grid frequency in both steady state and transients, typically with a storage reference power setpoint, $P^* = 0$ in (1). In this work, we consider the storage to be co-located with wind generation. We consider two options for the structure of the co-location, which are referred to as an outer VSG implementation (VSGo) and an inner VSG implementation (VSGi) in this paper, which are shown in Fig. 2 and Fig. 3 respectively.

2.2 Outer VSG implementation

In this case, VSG control is implemented into the converter, interfaced directly to the ESS and the ESS is co-located with renewable energy sources, i.e. Wind Turbine

Generation (WTG) as in Fig. 2. The advantage of this topology is that there is no modification required for the original WTG system, for which the Grid-tied converter (G-converter) still works in grid-following mode with outer power inner current control. This is, of course, a feasible and economical means to co-locate VSG controlled storage with existing renewable energy sources. However, the VSG control in this topology only acts as a support to the generation providing emulated inertia (1), droop control (2) and voltage regulation (3). The generated power from the WTG does not go through the swing equation (1), so that the VSG introduces no damping to the generated wind power conversion. Consequently, in this configuration, the dynamics arising from stochastic wind would increase the corresponding frequency variations especially in a WTG dominated system.

2.3 Inner VSG implementation

In this case, the VSG control is implemented into the G-converter of the WTG as shown in Fig. 3, and the ESS connects to the DC link of the WTG system via the E-converter which implements the DC voltage control. In this topology, the entire VSG-controlled WTG system moves from being grid-following to grid-forming. The generated power goes through the swing equation with inertia and damping via the VSG-controlled G-converter to the grid. Thus, the dynamics from stochastic wind are filtered, and the power injection to the grid is much smoother. Note, the mismatched power between the generation and grid injection is supplied or stored by the ESS.

3 Case Study: All-Island Irish Transmission System

In this section, the VSG control strategies discussed above are implemented and tested with the AIITS, which represents a leading example of a relatively rapid move towards a power system operated with high penetration of CIG. Presently with approximately 32% average electricity generation from wind energy, the system is instantaneously operated with up to 65% non-synchronous penetration [49]. With recently announced targets of achieving an average of 70% electricity generation from renewables by 2030 [50], the system will be required to operate with much higher

instantaneous levels of non-synchronous generation, the majority coming from on-shore and off-shore wind and PV [51].

The AIITS consists of 1,479 buses, 1,851 transmission lines and transformers, and 245 loads. It has a very limited transmission capacity to other systems as it is only interconnected with the UK via two HVDC interconnectors, the largest of which is a 500 MW VSC based HVDC link [52] which also represents the largest infeed to the system. If this UK interconnector fails unexpectedly (the largest infeed outage), the backup power relies on the local reserve and in this context, the fast frequency response control scheme of the CIG is crucial to maintain the power balance of the system.

The transition from the conventional SG-based generation to the converter-based generation with high renewable penetration will decrease the system inertia and potentially result in stability issues. The Irish TSO, EirGrid, requires that the frequency deviation shall remain within 50±0.2 Hz under normal operation, while it shall remain within 50±2 Hz, with RoCoF limited to 1 Hz/s in the first 500 ms [53] after a contingency. Therefore, the application of the VSG control in the existing ESS and planned WTG systems would be of great importance to the system stability. In fact, the importance of such response is already recognized by the TSO as evidenced by the recent introduction of a fast frequency response product [54]. The important question being investigated here is whether the system would maintain the same stability level if it migrates to the 100% CIG.

Since 80% of renewable electricity in Ireland is generated from wind, the VSG control is only considered to be implemented into the WTG system. The VSG-controlled WTG system is modeled as in Figs. 2 or 3, where the wind turbine used is a Full Converter Wind Turbine (FCWT) model [55]. The storage model is simplified as a constant DC voltage source with power limits. The VSG is modelled as equation (1-10) and this model has been verified via hardware experiment in our previous work

[46]. The AIITS dynamic model is built in Dome, a Python-based power system software tool [56] using data provided by EirGrid. There are 21 conventional synchronous power plants, which reflect the conventional generation portfolio in Ireland which consists of 5 coal, 10 gas, 4 hydro and 2 distillate plants [57]. Each plant is modelled as a single SG with individual AVR and TG controls, using 6th order synchronous machine models. Due to reasons of commercial sensitivity, the dynamic parameters of the generators are not exactly those used in practice but are based on generic generator models of the generator technology tuned to provide a close match with the actual system dynamics [58]. In addition to the conventional generators, there are 176 existing wind power plants, of which 142 are Doubly-Fed Induction Generator (DFIG) based and 34 are Constant Speed Wind Turbine (CSWT). Note, these 142 DFIGs uses conventional grid-following converters with constant power control and participate in primary frequency support with static droop control, while 34 CSWT do not participate frequency support. The largest generator, 288.52 MW in the system is set as a slack bus. In the following case study, all the generators are online. As a baseline scenario, we consider the situation where 50.77% of the generation is from the existing wind farms, i.e. 50.77% Wind Penetration (WP). The WP refers to the percentage of the total production being supplied by WTG in the initial state, i.e. before the disturbance. Note, the TSO currently allows the operation of the system with up to 65% non-synchronous penetration [59]. The grid frequency is measured by the central of inertia (COI). The time step of the simulation is 10 ms. The model provides a dynamic representation of the actual Irish electrical grid with accurate topology and load data and should reflect the real Irish system response.

Using the model above, the paper investigates the following aspects of the system-level impacts of the VSG:

1). The frequency stability in respect to the migration from the SG-dominated system to the 100% VSG-controlled CIG-dominated system in the event of a contingency (loss of largest infeed). Based on these results, the minimum quantity of

the ESS with VSG control required to ensure the stability of the system is investigated.

2). The frequency dynamics of the system under different WP scenarios, including a comparison of the different VSG configurations (VSGo as Fig. 2 or VSGi as Fig. 3) considering stochastic variation in wind generation and loads.

4 VSG-based Frequency Support in the AIITS

It could be argued that, since the virtual inertia implementation simply emulates the electromechanical behavior of the SG, then the VSG would be expected to have a similar performance to the SG during frequency transients after a contingency if the VSG settings are set identical to the SG characteristics. However, VSG control is applied to the power converter with a typical response time on the order of milliseconds, while the response of the SG and its primary control, TG, are much slower, i.e. on the order of seconds. Thus, the VSG could potentially provide faster frequency control and have better performance than the SG. On the other hand, the VSG compensated power is provided from the storage through a power converter, with binding current limits to avoid overcurrent, whereas the SG can tolerate overcurrent for a limited time. This restricts the quantity of emulated inertia, since the droop power and inertia power share the same power source and the same grid-tied interface. To be a fair comparison, the relevant parameters of the VSG control are set to be identical to that of the SG they replaced, i.e. virtual inertia is set identical to the SG inertia, the frequency-power droop gain is set identical to the TG gain, and the virtual impedance is set to the SG stator impedance. The capacity of the WTG system with the ESS is set to have the same power rating as the original SG with TG. The initial operation point is also set to be identical for the discussed devices. The VSC voltage and current controller parameters are set following the design approach for a voltage controlled VSC given in [60]. In the following analysis, two versions of the SG are used for the results. SG1 is the baseline case which uses the original SG data (TG time constant is in a range of 5-10 s). The SG2 case is a hypothetical case where it is

assumed that the SG can have a modified and fast TG response time of 0.1 s. The purpose of using SG2 is simply to provide a comparison between the inertial response from the VSG and an SG with similar characteristics. To illustrate the limitations of providing frequency support from the conventional grid-following CIG, a "Droop" case is also used, where the SG are replaced by a conventional grid-following WTG co-located with storage providing frequency support through a grid following droop control. In all cases, the VSGo and droop-controlled storage are co-located with a FCWT. Initially in this section, the wind input is set to be constant. The installed generation is 6.157 GW, while overall system load at this time is 2.36 GW, and the contingency which is the loss of the largest infeed, i.e. the HVDC line to the UK outage (400 MW), occurs at 1 s. Note this represents a relatively low loading scenario for the system, but something of a worst case in terms of disturbance as the loss of largest infeed represents the loss of a large portion of existing supply.

4.1 Case 1: device test

In order to better understand the full system-level results in later sections, we first show the response of a single device when it replaces a single SG in the baseline system. In this test, we compare the responses for each of the discussed devices, i.e. SG1 (baseline case), SG2, VSGi, VSGo and droop-controlled storage. In each case, the tested device replaces the SG keeping the same rating, 110 MW. Fig. 4 presents the grid frequency and device active power output after the HVDC interconnector outage at 1 s.

It can be seen from Fig. 4 that the lowest grid frequency nadir in this test occurs for the SG1, where the TG is set generally in second-time scale. Although the SG1 can provide the inertia (see the instant 1 s at Fig. 4 (b)), due to the slow TG reaction, the transient power compensation is less (1~8 s in Fig. 4 (b)). The droop response verifies that the power converter can have a much faster droop response, but, due to the absence of the inertia, it follows the frequency variation and therefore leads to the lower nadir in the grid frequency. The VSGs clearly combines the fast droop response

with an inertial response. The frequency support function, i.e. the frequency to power loop, of the VSGi and VSGo are identical, therefore, the VSGi and VSGo have the same response to the contingency. The response is also similar to that of the SG2, which highlights the fact that in terms of frequency response the VSG acts like an SG with fast TG but otherwise similar settings

For these results, only a single SG has been replaced in the system and therefore the different device responses make only a small difference in the overall system frequency behavior as indicated by the different curves in Fig. 4(a). However, from the results in Fig. 4(b) it can be anticipated that the widespread replacement of SG by VSG might improve overall system frequency response, due to the similar inertial response but faster droop response.

The next subsection investigates the system frequency response as all the SG are replaced by VSG, corresponding to a system with greater levels of generation from wind farms.

4.2 Case 2: Possibility of 100% Renewable Penetration

In this test, we increase the WP in the system by gradually replacing the SG by VSG all the way to achieving a fully non-synchronous system where all of the generation is provided from the wind. When replacing the SG, three types of wind farm and storage control is considered, the inner (VSGi), the outer VSG (VSGo) and the grid following with droop. For each case, the frequency behavior of the system in response to the contingency is obtained similar to the result in Fig. 4 (a).

Fig. 5 compares the system frequency in a 100% WP situation under the different control approaches to the original system frequency response (SG1). As expected, the VSG dominated system shows an improved frequency response compared to the original system (SG1) with the enhancement of the frequency nadir from 49.26 Hz to 49.68 Hz, while the droop-controlled case is unstable. The VSGo and VSGi as expected have identical responses.

Fig. 6 records the resulting frequency nadir and RoCoF measured at 500 ms after the contingency for each case. Compared with the original system, due to the faster response of the VSG as indicated in Fig. 4(b), the increase of the VSG-controlled WTG improves the overall system frequency transients both in terms of improved nadir and RoCoF. However, the droop-controlled storage plus WTG system, due to the reduction of the overall system inertia, worsens the system transients, resulting in a significant increase in the RoCoF, with the system becoming unstable when the WP increases to 80%. The comparison with the droop case simply highlights the importance of the virtual inertia which has been shown in previous works [40][46].The main result is that the VSG-controlled WTG can facilitate 100% WP actually with improved frequency stability, at least under the assumption of similarly rated VSG, compared to the system with SG.

4.3 Case 3: Level of ESS Frequency Response

The previous section established that in the 100% WP situation, after the contingency, compared with the original SG dominated system, the Irish system is improved by the inclusion of the VSG control with lower frequency nadir at 49.67 Hz and RoCoF at 0.31 Hz/s. However, in that case, the inertial response and primary reserve power capacity come entirely from the ESS. Due to the improved frequency response, the level of response provided by the VSG could be reduced which would allow a reduction in the ESS power rating, thus potentially saving capital cost. To investigate the potential for reduction of the ESS power capacity, we take the 100% WP situation and gradually reduce the level of frequency support (i.e. the droop gain is reduced in 5% steps) from the ESS and again observe the frequency nadir and RoCoF. Note here the reduction in droop gain can be viewed as a reduction in the reserve in relation to the TG gain reduction from the baseline case SG1. Considering, however that the inertial and droop power share the same power source, if a reduction in ESS rating is to be achieved then to avoid the converter hitting its rated power limit , both the inertia and droop gain must be reduced. Previous work [35, 61] has shown that the terminal response of the VSG can be approximated by a second

order response with a damping ratio which is directly proportional to droop gain and inversely proportional to the square root of inertia setting. Hence in order to preserve the terminal response damping ratio, the inertia is reduced proportionally to the square root of the droop gain [61].

Fig. 7 records the frequency transients during this process, where for comparison, the frequency nadir and RoCoF from the original baseline system (55% WP) with reduced TG gain are also shown. It should be noted that in this scenario, the online SG inertia remains constant and is independent on the droop response. It can be seen that the reduction gives a lower frequency nadir after the contingency in all scenarios. The primary reserve reduction has no effect on the RoCoF for the SG1 scenarios, as the inertia in the SG dominated system is unchanged. Meanwhile, in the VSG dominated system, the inertia must also reduce as it is limited by the reduced ESS power capacity. The Irish grid code now requires that the RoCoF should be limited to 1 Hz/s in the first 500 ms, and that the frequency deviation should be within ±2 Hz. Considering these grid code requirements, the response reduction is first constrained by the RoCoF at 20% of the original capacity. Of course, if the system is operated to maintain the same frequency nadir or RoCoF as in the original SG dominated system, then the response can only be reduced to 45% or 60% of the original respectively.

Fig. 8 presents the frequency transients after the contingency for all reduced response values at all steps. It can be seen that the gap between each step is increasing with the ESS response decrease. This is also reflected in Fig. 7, where the frequency nadir and RoCoF for the VSG dominated system become exponentially worse with the response reduction. In addition, the response reduction in the VSG dominated system, although adequate to ride through the transients, has a negative impact on the steady-state frequency deviation as would be expected from a reduced steady-state droop response. If the system is required to maintain the same steady-state frequency deviation under primary control as the original system, then the droop should maintain the same volume as the original.

5 Frequency Variation under VSG Generation

For the previous investigation of frequency stability from the VSG, the generation power from the wind was assumed constant. For the VSG, the generated power comes from the wind farms and therefore obviously has variability. The co-located ESS can, of course, mitigate this variability. However as indicated in Section II, the structure of the co-located wind turbine and ESS may be expected to have an influence on the VSG-controlled WTG system generation. In the VSGi system, the variable generated wind power is fed to the grid via the VSG-controlled converter interface and thus damped, due to the emulated swing equation, while for the VSGo system, the generated wind power directly feeds into the grid with no damping contribution. The VSG controlled co-located ESS in this case only reacts to the resulting grid frequency variations. This difference leads to different frequency dynamic characteristics in the two cases. This section investigates the frequency variations from these two VSG-controlled WTG topologies in the low WP (50.77%) and high WP (100%) cases. For this analysis, the wind input is now set to be stochastic using a Weibull distribution model and the simulation is run 100 times for each case. The average value and variance of the frequency are analyzed in the results.

5.1 Case 4: Frequency variation in the 50.77% WP system

In this case, the system is the same as in case 1 with 50.77% WP, where only one SG is replaced by the tested device (VSGo and VSGi) with 110 MW initial generation. The objective here is just to compare the output from a single device so as to better understand the later results for the system. Thus, in order to make a clearer comparison between VSGo and VSGi, only the discussed single VSG-controlled WTG system has the stochastic wind applied while the others still have constant wind. Fig. 9 compares the total power output between the VSGo and VSGi systems and Fig. 10 presents the system frequency for the VSGo and VSGi scenarios.

It can be seen from Fig. 10 that the frequency response is very similar in these two

VSG configurations with a variance of 0.008 Hz. However, Fig. 9 verifies that the virtual inertia and damping from the swing equation smooths the VSGi active power output, compared to the VSGo scenario. Thus, the similar system frequency response is because there is only one such device in the system. In other words, if the penetration of VSGi increased in the system, the benefit of the damped power generation would be anticipated to be greater, resulting in lower frequency variations.

5.2 Case 5: Trade-off between VSGo and VSGi

In this case, the tested system is the same as in case 2 with 100% WP, where all of the SGs are replaced by either VSGo or VSGi devices. The wind speeds for all wind turbines used in the system (VSGo, VSGi, and existing 142 DFIGs and 34 CSWTs) are now changed to have a stochastic variation. In addition, the system loading is also changed to have stochastic variations where the load stochastics are modeled by the Ornastein-Uhlenbeck's process [62] with ±5% of variation to their original values. Keeping in mind that the system frequency is to be kept within ±0.2 Hz frequency variation, this section quantifies the relationship between the frequency variance (due to stochastic wind and load) and the penetration of the VSGi vs VSGo in the system under the 100% WP scenario. For this study, the system starts with all of the added WTGs being of the VSGo structure, and these are then gradually changed to the VSGi structure with all being VSGi at the end. Fig. 11 presents the grid frequency variations under pure VSGo and VSGi situations. Fig. 12 records the variance for all tests as a percentage of the VSGi generation to the whole system generation with the 0.2 Hz standard marked as a black dashed line in the figure.

It can be seen from Fig. 11, as expected, compared with the VSGo scenarios, the VSGi scenarios have significantly improved the system frequency dynamics, with a reduction in variance from 0.26 Hz in the VSGo case to 0.13 Hz in the VSGi case, i.e. a 50% reduction. Installation of only the VSGo to achieve the 100% WP does not ensure the meeting of the ±0.2 Hz frequency variation tolerance. On the other hand, using

the VSGi topology can satisfy the standard. However, as mentioned earlier, considering costs a mixed combination of both approaches may be better. With this consideration, Fig. 12 indicates that if at least 8% of the total capacity consists of VSGi, the system frequency deviation would satisfy the standard.

6 Conclusions

The paper evaluates power system frequency dynamics, under VSG control of co-located wind and storage as a solution to achieving a 100% CIG system operation. The Irish power system is used as a realistic case study, consisting as it does, of a system with relatively high levels of existing conventional, grid feeding WTG, and with no synchronous interconnection to larger systems.

Based on the results, the following conclusions are relevant.

1) In principle for this case study of a realistic system, it is possible to have a stable system with improved frequency dynamics in a 100% CIG system with VSG control of storage co-located with wind generators. Under the pure grid-following control of wind turbines with additional droop-based frequency support from storage, the system will become unstable significantly before the 100% CIG scenario, in this case study, at approximately 80% CIG penetration.

2) Due to the faster response of the converters, the replacement of SG by VSG could result in improved frequency stability compared to the original SG dominated system. The advantage could be taken of the improved frequency response, to reduce the level of response provided and hence the ESS power rating required in the VSG dominated system, e.g. to 45% of the original in Ireland. However, it is important to note that because the inertia and droop power share the same power source, the ESS power rating reduction reduces the system inertia, so that eventually RoCoF limits the reduction possible, e.g. to 60% in Ireland case study. On the other hand, if it

considers the steady-state frequency deviation, the droop power should remain in the same level as using TG in the SG dominated system.

3). From the perspective of supplying virtual inertia in the system, the outer ESS WTG system (VSGo) and the inner ESS WTG system (VSGi) provide a similar response. However, in terms of smoothing the frequency variations from varying wind, the VSGi is damped and smoother than the VSGo. This has a significant difference in the high WP system and, in particular, the VSGi results in significantly reduced frequency deviations due to the stochastic variation of load and wind. The more VSGi devices in the system, the smaller the frequency deviations and for example in the 100% WP Irish system, at least 8% of the total WTG capacity should be installed as VSGi in order to keep the frequency variation within a 0.2 Hz band.

Although the case study used here is very much focused on the Irish power system, we believe that all of the above conclusions are relevant to any power system as it transitions to the use of 100% CIG.

In summary this paper indicates that the VSG is an option to replace the SG in order to achieve higher CIG penetration while maintaining the system stability. However, it is realized that there are several issued related to 100% CIG penetration which the study does not directly address and which are considered for future work. For example, it is also known that voltage stability issues are equally important in the case of high penetration of CIG [37] and that a suitable control approach for reactive power provision should be provided. However, this aspect is deemed beyond the scope of this work. It should also be noted that the modelling of the system in this work is fundamental frequency modelling, which typically neglects line dynamics. On the other hand, it is known that due to fast dynamics of the CIG there can be interactions between the converter and line dynamics which give rise to higher frequency oscillations, which can only be revealed by detailed EMT modelling. These oscillations can be avoided or damped at the device control level by proper choice of

VSG parameters or by the inclusion of virtual resistance [35]. In addition, as it is unlikely that all CIG in a system will be controlled as a VSG the question of the required slit between grid forming and grid following arises. Note in this study as the baseline case has approximately 50% of the generation coming from the existing grid following converters, the 100% CIG scenario represents a situation where these is approximately a 50:50 split between grid following and grid forming converters. Other studies have suggested that the percentage of grid forming could be lower, e.g. 30% [16], but the determination of this percentage has not been a focus of this study. Future work should investigate these issues in a more comprehensive study which should also include investigations under different loading and wind generation scenarios.

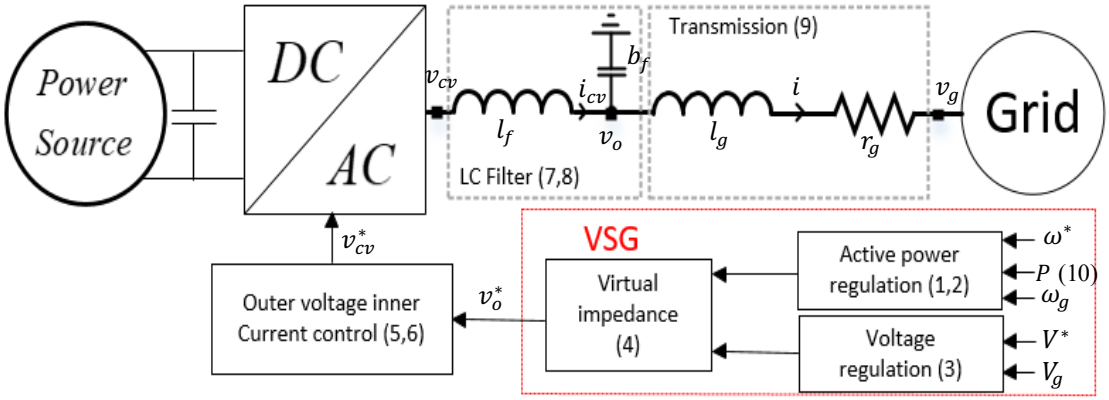

Fig. 1. VSG control structure

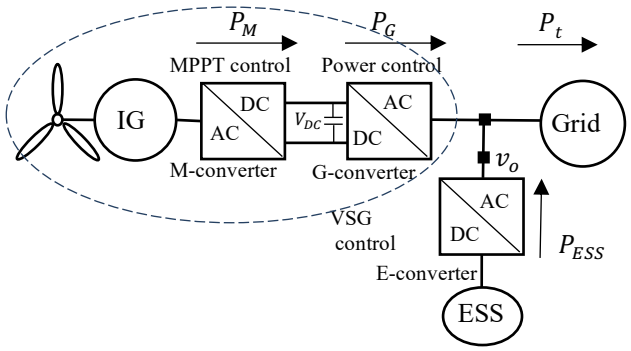

Fig. 2. VSGo system

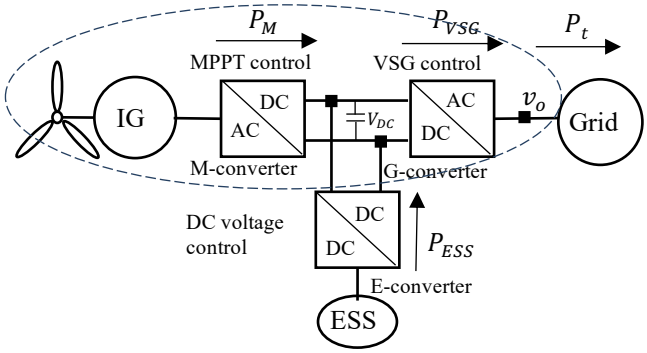

Fig. 3. VSGi system

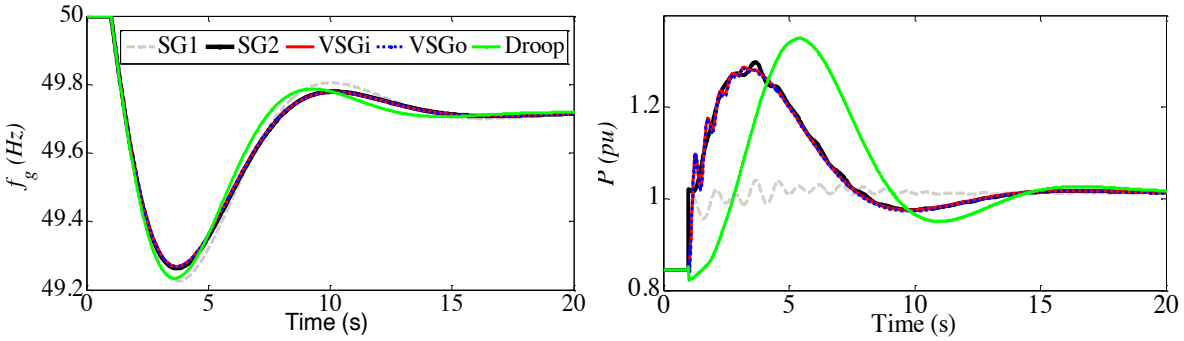

(a) Grid frequency

(b) Device active power

Fig. 4. Case 1: Single device test

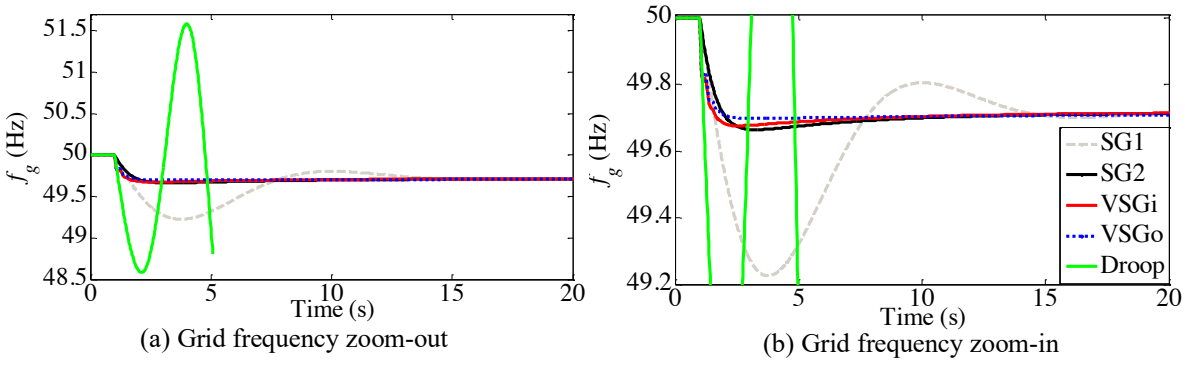

(a) Grid frequency zoom-out

(b) Grid frequency zoom-in

Fig. 5. Case 2: 100% wind penetration

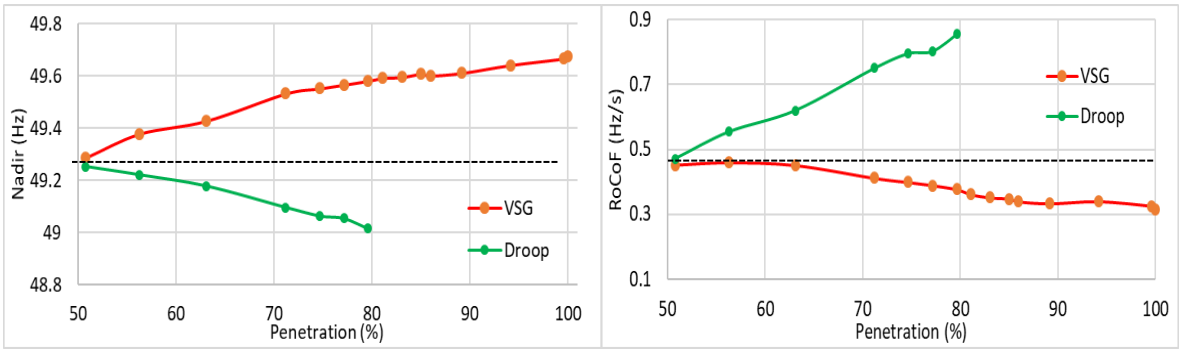

(a) Frequency nadir VS. wind penetration (b) RoCoF VS. wind penetration

Fig. 6. Frequency transient response VS. wind penetration increase

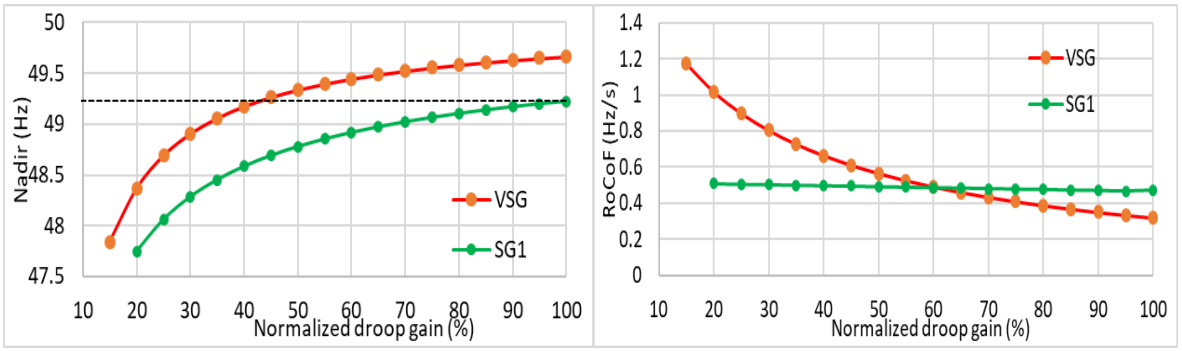

(a) Frequency nadir VS. reserve reduction (b) RoCoF VS. reserve reduction

Fig. 7. Frequency transient response VS. ESS rating reduction

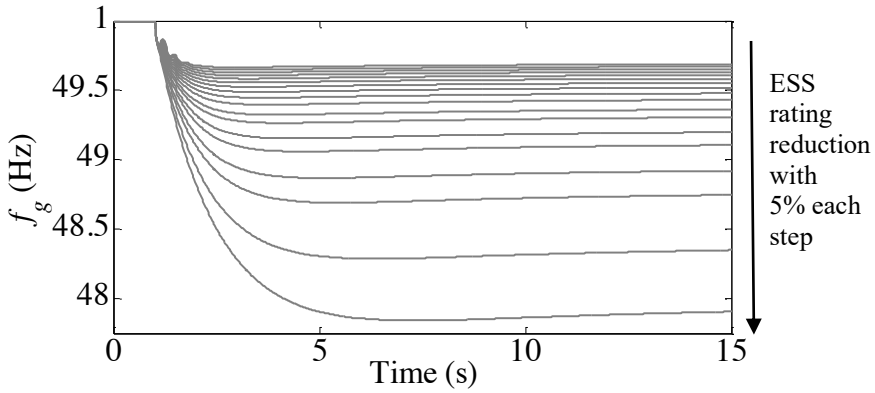

Fig. 8. Case 3: ESS rating reduction

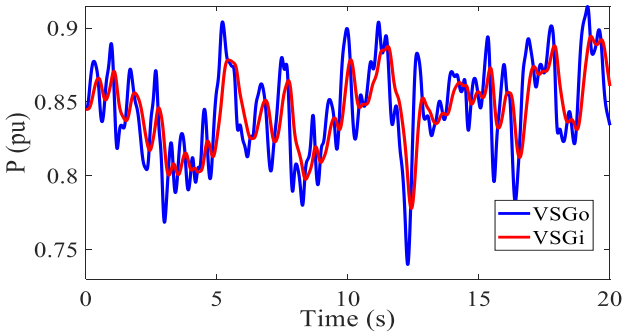

Fig. 9. Case 4: WTG system total generation

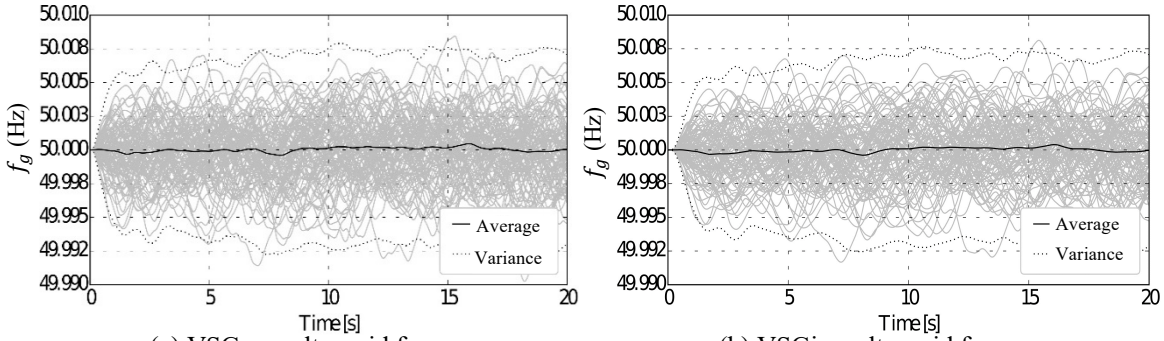

(a) VSGo result – grid frequency (b) VSGi result – grid frequency

Fig. 10. Case 4: Grid frequency in the 50.77% WP system

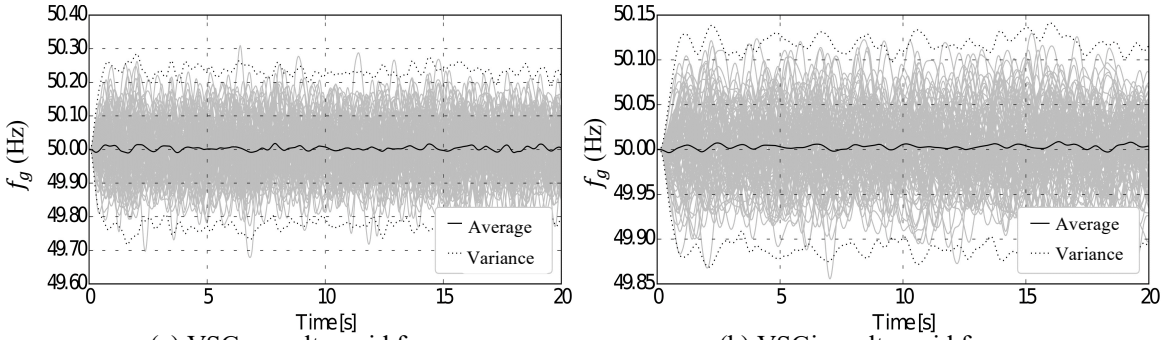

(a) VSGo result – grid frequency (b) VSGi result – grid frequency

Fig. 11. Case 5: Stochastic generation and load under 100% WP

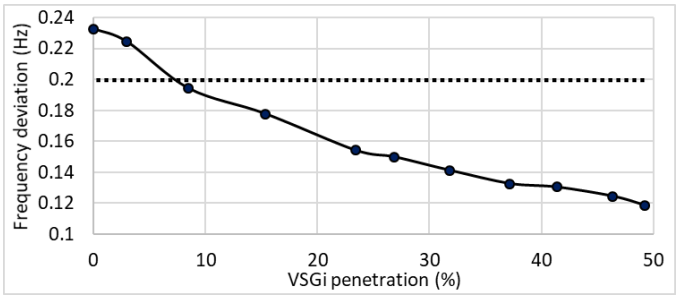

Fig. 12. Case 6: VSGi penetration vs. frequency deviation

Acknowledgements

This work is funded by the Science Foundation Ireland (SFI) Strategic Partnership Programme Grant Number SFI/15/SPP/E3125 and SFI/15/IA/3074.

References

[1] J. Quintero, V. Vittal, G. T. Heydt and H. Zhang, "The Impact of Increased Penetration of Converter Control-Based Generators on Power System Modes of Oscillation," *in IEEE Transactions on Power Systems*, vol. 29, no. 5, pp. 2248-2256, Sept. 2014.

[2] A. Božiček, *et al.*"Deliverable 5.4Influence of PQ disturbances on operation of PE rich power networks," MIGRATE-Massive InteGRATion of power Electronics devices, Dec. 2018.

[3] W. R. Tarnate, *et al.* "D1.2 Requirements placed on energy systems on transition to 100% RES," RESERVE, D1.2, v1.0, Sep. 2017.

[4] F. Milano, F. Dörfler, G. Hug, D. J. Hill and G. Verbič, "Foundations and Challenges of Low-Inertia Systems (Invited Paper)," 2018 Power Systems Computation Conference (PSCC), Dublin, 2018, pp. 1-25.

[5] T. Ackermann, T. Prevost, V. Vittal, A. J. Roscoe, J. Matevosyan, and N. Miller, "Paving the Way: A Future Without Inertia Is Closer Than You Think," *IEEE Power Energy Mag*., vol. 15, no. 6, pp. 61-69, 2017.

[6] J. O'Sullivan, A. Rogers, D. Flynn, P. Smith, A. Mullane and M. O'Malley, "Studying the Maximum Instantaneous Non-Synchronous Generation in an Island System—Frequency Stability Challenges in Ireland," in *IEEE Transactions on Power Systems*, vol. 29, no. 6, pp. 2943-2951, Nov. 2014.

[7] P. Tielens and D. V. Hertem, "The relevance of inertia in power systems," *Renewable and Sustainable Energy Reviews*, vol. 55, pp. 999-1009, 3 2016.

[8] F. Wilches-Bernal, J. H. Chow, and J. J. Sanchez-Gasca, "A Fundamental Study of Applying Wind Turbines for Power System Frequency Control," *IEEE Trans. Power Syst*., vol. 31, no. 2, pp. 1496-1505, Mar. 2016.

[9] Y. Liu, L. Zhu, L. Zhan, J. R. Gracia, T. J. King and Y. Liu, "Active power control of solar PV generation for large interconnection frequency regulation and oscillation damping," *International Journal of Energy Research*, vol. 40, pp. 353-361, 2016.

[10] Matej Krpan, Igor Kuzle, Dynamic characteristics of virtual inertial response provision by DFIG-based wind turbines, *Electric Power Systems Research*, Volume 178, 2020, 106005.

[11] G. Delille, B. Francois and G. Malarange, "Dynamic Frequency Control Support by Energy Storage to Reduce the Impact of Wind and Solar Generation on Isolated Power System's Inertia," *IEEE Transactions on Sustainable Energy*, vol. 3, pp. 931-939, 10 2012.

[12] B. Tamimi, C. Canizares and K. Bhattacharya, "System Stability Impact of Large-Scale and Distributed Solar Photovoltaic Generation: The Case of Ontario, Canada," *IEEE Transactions on Sustainable Energy*, vol. 4, pp. 680-688, 7 2013.

[13] M. F. M. Arani and E. EI-Saadany, "Implementing Virtual Inertia in DFIG-Based Wind Power Generation," *IEEE Trans. Power Sys.* Vol. 28, no. 2, May 2013.

[14] J. Ma, Z. Song, Y. Zhang, Y. Zhao and J. S. Thorp, “Robust Stochastic Stability Analysis Method of DFIG Integration on Power System Considering Virtual Inertia Control,” *IEEE Trans. Power Sys*. Vol. 32, no. 5, Sep. 2017.
[15] J. Ma, Y. Qiu, Y. Li, W. Zhang, Z. Song and J. S. Thorp, “Research on the Impact of DFIG Virtual Inertia Control on Power System SmallSignal Stability Considering the Phase-Locked Loop,” *IEEE Trans. Power Sys*. Vol. 32, no. 3. May 2017.
[16] J. T. Hennig, *et al.,* “Deliverable D1.5 Power system risk analysis and mitigation measures,” MIGRATE, vol. Sep, no. 15, 2019.
[17] Q.-C. Zhong and G. Weiss, “Synchronverter: Inverters that mimic synchronous generators,” *IEEE Trans. In. Electron*., vol. 58, no. 4, pp. 1259-1267, Apr. 2011.
[18] Q.-C. Zhong, P.-L. Nguyen, Z. Ma, and W. Sheng, “Self-synchronized synchronverters: Inverters without a dedicated synchronization unit,” *IEEE Trans. Power Electron*., vol. 29, no. 2, pp. 617-630, Feb. 2014.
[19] S. D’Arco, J. A. Suul and O. B. Fosso, "A Virtual Synchronous Machine implementation for distributed control of power converters in Smart Grids," *Electric Power Systems Research*, Vol. 122, pp. 180-197, May 2015.
[20] O. Mo, S. D’Acro and J. Suul, “Evaluation of Virtual Synchronous Machines with Dynamic or Quasi-Stationary Machine Models”, *IEEE Transactions on Industrial Electronics*, Vol. 64, no. 7, Jul. 2017.
[21] T. Kerdphol, F. S. Rahman, M. Watanabe, Y. Mitani, D. Turschner and H. Beck, "Enhanced Virtual Inertia Control Based on Derivative Technique to Emulate Simultaneous Inertia and Damping Properties for Microgrid Frequency Regulation," in *IEEE Access*, vol. 7, pp. 14422-14433, 2019.
[22] Y. Cao, *et al.*, "A Virtual Synchronous Generator Control Strategy for VSC-MTDC Systems," in *IEEE Transactions on Energy Conversion*, vol. 33, no. 2, pp. 750-761, June 2018.
[23] J. Fang, H. Li, Y. Tang and F. Blaabjerg, "Distributed Power System Virtual Inertia Implemented by Grid-Connected Power Converters," in *IEEE Transactions on Power Electronics*, vol. 33, no. 10, pp. 8488-8499, Oct. 2018.
[24] L. Huang *et al.*, "A Virtual Synchronous Control for Voltage-Source Converters Utilizing Dynamics of DC-Link Capacitor to Realize Self-Synchronization," in *IEEE Journal of Emerging and Selected Topics in Power Electronics*, vol. 5, no. 4, pp. 1565-1577, Dec. 2017.
[25] Q.-C. Zhong, “Virtual Synchronous Machines: A unified interface for grid integration,” *IEEE Power Electronics Magazine*, Vol. 3, Issue. 4, Dec. 2016.
[26] Q.-C. Zhong, Z. Ma, W. L. Ming, and G. C. Konstantopoulos, “Grid-friendly wind power systems based on the synchronverter technology,” *Energy Convers. Manage.* , vol. 8, no. 9, pp. 719-726, 2015.
[27] Y. Ma, W. Cao, L. Yang, F. Wang, and L. M. Tolbert, “Virtual Synchronous Generator Control of Full Converter Wind Turbines With Short-Term Energy Storage,” *IEEE Trans. Industrial Electronics*, vol. 64, no. 11, Nov. 2017.
[28] W. L. Ming and Q.-C. Zhong, “Synchronverter-based transformerless PV inverters,” in Proc. 40th Annu. Conf. IEEE Industrial Electronics Society (IECON 2014), Dallas, TX, pp. 4396-4401.
[29] S. Mishra, D. Pullaguram, S. Achary Buragappu and D. Ramasubramanian, "Single-phase synchronverter for a grid-connected roof top photovoltaic system," in *IET Renewable Power Generation*, vol. 10, no. 8, pp. 1187-1194, 9 2016.
[30] J. A. Suul, S. D’Arco, and G. Guidi, “Virtual Synchronous Machine-Based Control of a Single-Phase Bi-Directional Battery Charger for Providing Vehicle-to-Grid Services,” *IEEE Trans. Industry Applications*, vol. 52, no. 4, Jul/Aug. 2016.
[31] D. Chen, Y. Xu and A. Q. Huang, “Integration of DC Microgrids as Virtual Synchronous Machines Into the AC Grid,” *IEEE Trans. Industrial Electronics*, Vol. 64, no. 9, Sep. 2017.
[32] U. Agrawal, J. O’Brien, A. Somani, T. Mosier and J. Dagle, “A Study of the Impact of Reduced Inertia in Power Systems,” Proceedings of the 53rd Hawaii International Conference on System Sciences, 2020.
[33] Tayyebi, Ali, et al. "Interactions of Grid-Forming Power Converters and Synchronous Machines--A Comparative Study." arXiv preprint arXiv:1902.10750, 2019.

[34] D. Groß, M. Colombino, J. Brouillon and F. Dörfler, "The Effect of Transmission-Line Dynamics on Grid-Forming Dispatchable Virtual Oscillator Control," *IEEE Transactions on Control of Network Systems*, vol. 6, no. 3, pp. 1148-1160, Sept. 2019.
[35] J. Chen and T. O'Donnell, "Parameter Constraints for Virtual Synchronous Generator Considering Stability," *IEEE Transactions on Power Systems*, vol. 34, no. 3, pp. 2479-2481, May 2019.
[36] T. Shintai, Y. Miura and T. Ise, "Oscillation Damping of a Distributed Generator Using a Virtual Synchronous Generator," *IEEE Transactions on Power Delivery*, vol. 29, no. 2, pp. 668-676, April 2014.
[37] E. Vittal, M. O'Malley and A. Keane, "A Steady-State Voltage Stability Analysis of Power Systems With High Penetrations of Wind," *IEEE Transactions on Power Systems*, vol. 25, no. 1, pp. 433-442, Feb. 2010.
[38] H. Wu and X. Wang, "Design-oriented transient stability analysis of grid-connected converters with power synchronization control," *IEEE Trans. Ind. Electron.*, vol. 66, no. 8, pp. 6473–6482, 2019.
[39] L. Zhang, L. Harnefors and H. Nee, "Power-Synchronization Control of Grid-Connected Voltage-Source Converters," *IEEE Transactions on Power Systems*, vol. 25, no. 2, pp. 809-820, May 2010.
[40] J. Liu, Y. Miura and T. Ise, "Comparison of Dynamic Characteristics Between Virtual Synchronous Generator and Droop Control in Inverter-Based Distributed Generators," in *IEEE Transactions on Power Electronics*, vol. 31, no. 5, pp. 3600-3611, May 2016.
[41] S. D'Arco and J. A. Suul, "Equivalence of Virtual Synchronous Machines and Frequency-Droops for Converter-Based MicroGrids," in *IEEE Transactions on Smart Grid*, vol. 5, no. 1, pp. 394-395, Jan. 2014.
[42] Z. Shuai, Y. Hu, Y. Peng, C. Tu and Z. J. Shen, "Dynamic Stability Analysis of Synchronverter-Dominated Microgrid Based on Bifurcation Theory," in *IEEE Transactions on Industrial Electronics*, vol. 64, no. 9, pp. 7467-7477, Sept. 2017.
[43] A. Fathi, Q. Shafiee and H. Bevrani, "Robust Frequency Control of Microgrids Using an Extended Virtual Synchronous Generator," in *IEEE Transactions on Power Systems*, vol. 33, no. 6, pp. 6289-6297, Nov. 2018.
[44] J. Liu, Y. Miura, H. Bevrani and T. Ise, "Enhanced Virtual Synchronous Generator Control for Parallel Inverters in Microgrids," in *IEEE Transactions on Smart Grid*, vol. 8, no. 5, pp. 2268-2277, Sept. 2017.
[45] W. Du, Q. Fu and H. F. Wang, "Power System Small-Signal Angular Stability Affected by Virtual Synchronous Generators," in *IEEE Transactions on Power Systems*, vol. 34, no. 4, pp. 3209-3219, July 2019
[46] J. Chen, M. Liu, C. O'Loughlin, F. Milano and T. O'Donnell, "Modelling, Simulation and Hardware-in-the-Loop Validation of Virtual Synchronous Generator Control in Low Inertia Power System," 2018 Power Systems Computation Conference (PSCC), Dublin, 2018, pp. 1-7.
[47] J. Chen, M. Liu, F. Milano and T. O'Donnell, "Placement of Virtual Synchronous Generator Controlled Electric Storage combined with Renewable Generation, PowerTech, Milano, Italy, 23-27 June 2019.
[48] C. Qi, K. Wang, G. Li, X. Jiang and Q. Zhong, "Application and Validation of Virtual Synchronous Machines in Power System Operation," IECON 2018 - 44th Annual Conference of the IEEE Industrial Electronics Society, Washington, DC, 2018, pp. 103-108.
[49] Ireland, "National Renewable Energy Action Plan, " Fourth Progress Report, Dec. 2017.
[50] Irish Wind Energy Association, "IWEA ENERGY VISION 2030 IWEA's National Energy and Climate Plan for Ireland in 2030," March. 2018.
[51] EirGrid, "Tomorrow's Energy Scenarios 2017 Planning our Energy Future," July 2017.
[52] N. Aparicio, et al. "Automatic under-frequency load shedding mal-oeration in power systems with high wind power penetration," *Elsevier*, May 23, 2016.
[53] EirGrid and SONI, "RoCoF Alternative & Complementary Solution Project, Phase 2 Study Report," 31 March, 2016.
[54] EirGrid and SONI, "DS3: Rate of Change of Frequency (ROCOF) Workstream," June, 2017.

[55] F. Milano, Power System Modelling and Scripting, Springer, London, August 2010.
[56] F. Milano, “A Python-based Software Tool for Power System Analysis,” IEEE PES General Meeting, Vancouver, Canada, 21-25 July 2013
[57] Eirgrid, “All-Island Generation Capacity Statement 2017-2026,” April 2017.
[58] M. A. Adib Murad, G. Tzounas, M. Liu, F. Milano, “Frequency Control Through Voltage Regulation of Power Systems Using SVC Devices,” IEEE PES General Meeting, Atlanta, GA, 4-8 August 2019.
[59] EirGrid and SONI, “Annual Renewable Energy Constraint and Curtailment Report 2017,” June 2018.
[60] A. Yazdani and R. Iravani, “Voltage-soured Converters in Power Systems,” WILEY IEEE PRESS, March 2010, ISBN: 978-0-470-521564.pp204-269.
[61] J. Chen and T. O'Donnell, "Analysis of virtual synchronous generator control and its response based on transfer functions," *IET Power Electronics*, vol. 12, no. 11, pp. 2965-2977, 18 9 2019.
[62] F. Milano and R. Zárate-Miñano, “A Systematic Method to Model Power Systems as Stochastic Differential Algebraic Equations,” *IEEE Transactions on Power Systems*, vol. 28, no. 4, pp. 4537-4544, Nov. 2013.